



Published in final edited form as:

Appl Physiol Nutr Metab. 2018 February ; 43(2): 123–130. doi:10.1139/apnm-2017-0404.

The role of suppression of hepatic SCD1 expression in the metabolic effects of dietary methionine restriction

Laura A. Forney,

Laboratory of Nutrient Sensing and Adipocyte Signaling, Pennington Biomedical Research Center, Baton Rouge, LA 70808, USA

Kirsten P. Stone,

Laboratory of Nutrient Sensing and Adipocyte Signaling, Pennington Biomedical Research Center, Baton Rouge, LA 70808, USA

Desiree Wanders,

Department of Nutrition, Georgia State University, Atlanta, GA 30302, USA

James M. Ntambi, and

Departments of Biochemistry and Nutritional Sciences, University of Wisconsin-Madison, Madison, WI 53706, USA

Thomas W. Gettys

Laboratory of Nutrient Sensing and Adipocyte Signaling, Pennington Biomedical Research Center, Baton Rouge, LA 70808, USA

Abstract

Dietary methionine restriction (MR) produces concurrent increases in energy intake and expenditure, but the proportionately larger increase in energy expenditure (EE) effectively limits weight gain and adipose tissue accretion over time. Increased hepatic fibroblast growth factor-21 (FGF21) is essential to MR-dependent increases in EE, but it is unknown whether the downregulation of hepatic stearoyl-coenzyme A desaturase-1 (SCD1) by MR could also be a contributing factor. Global deletion of SCD1 mimics cold exposure in mice housed at 23 °C by compromising the insular properties of the skin. The resulting cold stress increases EE, limits fat deposition, reduces hepatic lipids, and increases insulin sensitivity by activating thermoregulatory thermogenesis. To examine the efficacy of MR in the absence of SCD1 and without cold stress, the biological efficacy of MR in *Scd1*^{-/-} mice housed near thermoneutrality (28 °C) was evaluated. Compared with wild-type mice on the control diet, *Scd1*^{-/-} mice were leaner, had higher EE, lower hepatic and serum triglycerides, and lower serum leptin and insulin. Although dietary MR increased adipose tissue UCP1 expression, hepatic *Fgf21* messenger RNA, 24 h EE, and reduced serum triglycerides in *Scd1*^{-/-} mice, it failed to reduce adiposity or produce any further reduction in hepatic triglycerides, serum insulin, or serum leptin. These findings indicate that even when thermal stress is minimized, global deletion of SCD1 mimics and effectively masks many of the

Corresponding author: Thomas W. Gettys (Thomas.Gettys@pbrc.edu).

Conflict of interest statement

The authors report no conflicts of interest associated with this manuscript.

metabolic responses to dietary MR. However, the retention of several key effects of dietary MR in this model indicates that SCD1 is not a mediator of the biological effects of the diet.

Keywords

dietary intake; essential amino acids; animal models; indirect calorimetry; FGF21

Introduction

Stearoyl-coenzyme A desaturase-1 (SCD1) is the rate-limiting enzyme for biosynthesis of the long-chain monounsaturated fatty acids (e.g., C16:1 and C18:1) required in the first committed step of triglyceride synthesis (Miyazaki et al. 2000; Paton and Ntambi 2009). The liver is an important site of lipid synthesis, and over-expression of hepatic SCD1 has been linked to obesity and hepatic steatosis (Gutierrez-Juarez et al. 2006). In contrast, global deletion of SCD1 reduces serum and liver triglycerides (Flowers et al. 2012), but interestingly, *Scd1*^{-/-} mice are also hypermetabolic, obesity-resistant, and show enhanced insulin sensitivity (Ntambi et al. 2002). *Asebia* mice have a naturally occurring mutation of the SCD1 gene (Gates and Karasek 1965) and share the hypermetabolic phenotype of *Scd1*^{-/-} mice (Cohen et al. 2002). These findings indicate a link between SCD1 and increased energy expenditure (EE). Studies examining the metabolic responses to tissue-specific deletion of SCD1 from liver (Miyazaki et al. 2007), adipose tissue (Hyun et al. 2010), and skin (Sampath et al. 2009) suggest that the complex phenotype produced by global SCD1 deletion derives primarily from epidermal barrier defects that enhance thermal conductance and compromise lipid synthesis and export from the liver (Binczek et al. 2007; Flowers et al. 2012; Sampath et al. 2009).

Recent studies have shown that dietary methionine restriction (MR) produces a significant reduction in hepatic SCD1 expression in rats and mice (Ables et al. 2012; Hasek et al. 2013; Perrone et al. 2010). Given the similarities between the metabolic phenotype of *Scd1*^{-/-} mice and mice fed an MR diet, the present study was undertaken to assess whether MR-dependent downregulation of hepatic SCD1 was linked to specific components of the metabolic responses to the MR diet. Using wild-type (WT) and *Scd1*^{-/-} mice housed at temperatures that either stimulated (23 °C) or minimized (28 °C) adaptive thermogenesis, we report that even at 28 °C, *Scd1*^{-/-} mice on the control diet respond as if cold-stressed, with many of their responses mimicking the responses to dietary MR. This produces a phenotype that masks some but not all of the responses to dietary MR, and argues that SCD1 is not a critical mediator of the effects of dietary MR.

Materials and methods

Animals and diets

All experiments were reviewed and approved by the Penning-ton Biomedical Research Center Institutional Animal Care and Use Committee on the basis of guidelines established by the National Research Council, the Animal Welfare Act, and the Public Health Service Policy on the humane care and use of laboratory animals. The experiments were conducted

using 5–6-week-old male WT or *Scd1*^{-/-} mice (Ntambi et al. 2002) on a C57BL/6J genetic background. Diets were formulated as extruded pellets (Dyets Inc., Bethlehem, Pa., USA). Energy content of both control (CON) and MR diets were 15.96 kJ/g, with 18.9% of energy from fat (corn oil), 64.9% from carbohydrate, and 14.8% from a custom mixture of L-amino acids. The CON diet contained 0.86% methionine, while the MR diet contained 0.17% methionine, and both diets contained no cysteine. Food and water were provided ad libitum and lights were on 12 h/day from 0700 to 1900 h. Body composition was measured by nuclear magnetic resonance spectroscopy (Bruker MiniSpec, Billerica, Mass., USA) at weekly intervals, using calibration standards and protocols defined by the manufacturer.

Experimental protocol

Ten WT and 10 *Scd1*^{-/-} mice were singly housed in shoebox cages and adapted to the CON diet for 1 week. Thereafter, half the mice of each genotype were randomized to either CON or MR diet. The mice were housed at 23 °C for the first 5 weeks of the study, but were then moved to 28 °C for the final 5 weeks of the study. Food consumption was measured at weekly intervals by weighing the food provided at the beginning of each interval and subtracting the weight of unconsumed and wasted food at the end. The corn-cob bedding was sifted through wire mesh to retrieve and weigh any food removed from the hopper but not eaten. During the last week of housing at each temperature, EE was measured by indirect calorimetry using an Oxymax system (Columbus Instruments, Columbus, Ohio, USA). Mice were adapted to the metabolic chambers for 24 h prior to measurement of oxygen uptake ($\dot{V}O_2$) and carbon dioxide production ($\dot{V}CO_2$) for 48 h at 18-min intervals. After measurement of EE at 28 °C at the end of the study, mice were returned to their home cages for 3 days and then euthanized after a 4-h fast. Tissues were harvested and flash frozen in liquid nitrogen. Serum and tissues were stored at -80 °C until analysis.

Analysis of indirect calorimetry data

Respiratory quotient (RQ) was calculated as the ratio of $\dot{V}CO_2$ produced to $\dot{V}O_2$ consumed, and EE was then calculated as $\dot{V}O_2 \times (3.815 + (1.232 \times RQ)) \times 4.1868$. Group differences in EE (kJ/(mouse·h)⁻¹) were compared using ANCOVA by calculating least-squares means that accounted for variation in EE attributable to differences in lean mass, fat mass, activity, genotype, diet, and genotype \times diet interaction as described previously (Wanders et al. 2015). The least-squares means \pm SE of EE for the genotype \times diet combinations were compared using a 2-way ANOVA and the significance of the model effects and interaction was tested using residual variance calculated within the ANCOVA (Wanders et al. 2015).

Serum metabolite analysis

Serum adiponectin, insulin, and leptin were determined using enzyme-linked immunosorbent assays (Millipore, Billerica, Mass., USA).

Triglyceride assays

Serum and hepatic triglyceride content were determined via colorimetric assay (Cayman Chemicals; Ann Arbor, Mich., USA). Serum was assayed undiluted. Approximately 20 mg

of liver tissue was homogenized in 100 μ L of included buffer before analysis, with amounts of detected triglyceride adjusted to the amount of tissue used in the assay.

RNA isolation and quantitative real-time polymerase chain reaction

One microgram RNA was isolated from liver and inguinal white adipose tissue (IWAT) and used for measurement of *fibroblast growth factor-21 (Fgf21)*, *Scd1*, and *uncoupling protein-1 (Ucp1)* messenger RNA (mRNA) as previously described (Wanders et al. 2017). Expression of mRNA was normalized to the expression of cyclophilin (Wanders et al. 2017).

Protein extraction and immunoblotting—Protein lysates of brown adipose tissue (BAT) were prepared by homogenizing samples in immunoprecipitation buffer (150 mmol/L sodium chloride, 1 mmol/L EDTA, 1 mmol/L EGTA, 10 mmol/L Tris base, 1% Triton X-100, 0.5% NP-40, 1 mmol/L sodium orthovanadate, 40 mmol/L sodium fluoride, 10 mmol/L β -glycerophosphate, 2.5 mmol/L sodium pyrophosphate, and 1 \times protease inhibitor cocktail (Sigma–Aldrich)). Protein concentrations were quantified, and 30 μ g of protein for each sample were separated by sodium dodecyl sulfate - polyacrylamide gel electrophoresis then transferred to polyvinylidene fluoride membranes. Blots were developed using Amersham enhanced chemiluminescence (GE Healthcare Life Science). The UCP-1 antibody was described previously (Commins et al. 1999), and its expression was standardized to PDC-E2 (antibody from Santa Cruz; Dallas, Texas, USA).

To analyze protein expression of SCD1, microsomal fractions from liver tissue were prepared and used to measure diet-induced changes in SCD1 expression by Western blotting as previously described (Hasek et al. 2013). Liver microsomes from *Scd1*^{-/-} mice, as well as whole-cell extracts from COS cells transformed with a SCD1 expression construct were used as negative and positive blotting controls, respectively. β -Actin was blotted as a loading control for SCD1 expression. Band densities were analyzed using Image J (National Institutes of Health; Bethesda, Md., USA).

Statistical analysis

Response variables measured at each housing temperature were compared using a 2-way ANOVA, with genotype and diet as main effects in the model. Means of each variable were compared within rearing temperature using residual variance as the error term and the Bonferroni correction. Protection against Type I errors was set at 5%. The analysis was conducted using Graphpad Prism (La Jolla, Calif., USA).

Results

Analysis of the measured components of energy balance indicated significant effects of genotype, diet, temperature, and genotype \times diet \times temperature interactions (Fig. 1). For example, dietary MR produced a significant and comparable reduction in body weight (BW) in WT and *Scd1*^{-/-} mice housed at 23 $^{\circ}$ C. MR also reduced BW in WT mice housed at 28 $^{\circ}$ C, but not in *Scd1*^{-/-} mice (Fig. 1A). Compared with WT mice on the CON diet housed at 23 $^{\circ}$ C and 28 $^{\circ}$ C, adiposity was 26% and 19% lower in *Scd1*^{-/-} mice at the respective temperatures (Fig. 1B). Nevertheless, dietary MR produced comparable reductions in

adiposity in *Scd1*^{-/-} and WT mice housed at 23 °C, and a 17% reduction in adiposity in WT mice at 28 °C (Fig. 1B). However, as with BW, MR had no effect on adiposity of *Scd1*^{-/-} mice housed at 28 °C (Fig. 1B). The consumption rate of the CON diet was significantly higher in *Scd1*^{-/-} compared with WT mice housed at both temperatures, and dietary MR increased energy intake comparably in both genotypes at 23 °C (Fig. 1C). MR produced a significant 22% increase in intake in WT mice housed at 28°C, but MR failed to increase energy intake in *Scd1*^{-/-} mice at this temperature (Fig. 1C). As with energy intake, EE in mice on CON was 30% and 50% higher in *Scd1*^{-/-} mice than WT mice housed at 23 °C and 28 °C, respectively (Fig. 1D). In addition, EE was significantly lower in WT (e.g., 30%) and *Scd1*^{-/-} mice (e.g., 53%) housed at 28 °C compared with 23 °C (Fig. 1D). Despite these temperature-dependent differences, dietary MR produced significant increases in EE in WT and *Scd1*^{-/-} mice housed at either 23 °C or 28 °C (Fig. 1D). Voluntary activity did not differ between WT and *Scd1*^{-/-} mice, regardless of diet or housing temperature (data not shown).

With regard to thermogenic markers in adipose tissue, MR produced significant increases in UCP1 protein expression in BAT (Fig. 1E) and *Ucp1* mRNA expression in IWAT (Fig. 1F) of both WT and *Scd1*^{-/-} mice (Fig. 1E). Collectively, these findings show that the absence of SCD1 did not compromise the ability of dietary MR to increase EE or expression of thermogenic markers in mice housed near thermoneutrality. However, the ability of MR to reduce adiposity and BW accretion was compromised in *Scd1*^{-/-} mice housed at 28 °C but not 23 °C.

In mice housed at 28 °C, dietary MR was able to recapitulate its previously reported (Perrone et al. 2010; Hasek et al. 2013; Ables et al. 2012) reduction in hepatic *Scd1* mRNA in WT mice (Fig. 2A), and as expected *Scd1* mRNA was undetectable in *Scd1*^{-/-} mice. SCD1 protein expression was also measured after initially establishing the specificity of the antibody with whole-cell extracts of COS cells transduced with empty vector or an SCD1 expression vector (Fig. 2B). A protein migrating at the same molecular weight (37 kDa) as SCD1 was detected in liver microsomes from WT mice on each diet but not in *Scd1*^{-/-} mice (Fig. 2C). And as reported previously (Hasek et al. 2013), dietary MR produced a 4.5-fold decrease in SCD1 expression in WT mice (Fig. 2C). The MR-induced reduction in hepatic SCD1 expression was associated with a 30% reduction in serum (Fig. 2D) and liver triglyceride in WT mice (Fig. 2E). In the comparison of WT and *Scd1*^{-/-} mice on the CON diet, serum triglyceride was 20% lower in *Scd1*^{-/-} mice and MR produced a further 27% decrease in triglyceride levels in *Scd1*^{-/-} mice (Fig. 2D). Liver triglyceride levels were 3-fold lower in *Scd1*^{-/-} compared with WT mice, and dietary MR produced no further reduction in liver triglycerides (Fig. 2E).

Previous studies established that in mice housed at 23 °C, dietary MR increases hepatic *Fgf21* mRNA (Perrone et al. 2010; Stone et al. 2014) and serum adiponectin, and decreases serum insulin and leptin (Malloy et al. 2006; Hasek et al. 2010). We found that all of these responses were intact in WT mice housed at 28 °C, with dietary MR increasing hepatic *Fgf21* mRNA by 4.5-fold (Fig. 3A), serum adiponectin by 1.7-fold (Fig. 3B), and decreasing serum insulin by 4.5-fold (Fig. 3C) and serum leptin by 3.7-fold (Fig. 3D). A genotype-specific effect was detected in WT and *Scd1*^{-/-} mice on the CON diet, with hepatic *Fgf21* mRNA, serum insulin, and serum leptin being significantly lower in *Scd1*^{-/-} compared with

WT mice (Figs. 3A, 3C, 3D). Dietary MR produced a 4-fold increase in hepatic *Fgf21* mRNA in *Scd1*^{-/-} mice (Fig. 3A), but the diet was without further effect on serum adiponectin, insulin, or leptin in *Scd1*^{-/-} mice (Figs. 3B, 3C, 3D). Viewed collectively, these findings illustrate genotype-dependent effects on insulin and leptin that are directionally aligned with the expected responses to the diet. The failure of dietary MR to produce further significant decreases in insulin or leptin, or to increase adiponectin, produced genotype by diet interactions for all responses except the induction of hepatic FGF21.

Discussion

SCD1 is the rate-limiting enzyme in the synthesis of the mono-unsaturated fatty acids required for synthesis of membrane phospholipids, cholesterol esters, and triglyceride (Paton and Ntambi 2009). The enzyme is widely expressed across tissues, and targeted disruption of the gene across multiple tissues produces a complex phenotype involving organ-specific changes in lipid metabolism. Global deletion or targeted disruption of SCD1 in the skin compromises function of the epidermal lipid barrier (Dobrzyn et al. 2004; Miyazaki et al. 2000, 2001*b*; Ntambi et al. 2002; Rahman et al. 2005; Sampath et al. 2009), and the diminished insulation accentuates heat loss through the skin and activates thermoregulatory thermogenesis. The result is mice that are hyperphagic, hyper-metabolic, resistant to diet-induced obesity, and have lowered triglycerides and increased insulin sensitivity (Binczek et al. 2007; Lee et al. 2004; Ntambi et al. 2002). In contrast, tissue-specific deletion of SCD1 from the liver (Miyazaki et al. 2007), adipose tissue (Hyun et al. 2010), or both (Flowers et al. 2012) produces mice with predictable organ-specific changes in long chain fatty acid metabolism and subtle metabolic changes that do not alter energy balance or prevent diet-induced obesity. The phenotype of global *Scd1*^{-/-} mice mirrors the metabolic phenotype produced by dietary MR in rodents (Hasek et al. 2010; Wanders et al. 2015), and interestingly, dietary MR also produces a profound reduction in hepatic SCD1 protein expression (Hasek et al. 2013). Therefore, a key goal of the present work was to determine whether the absence of SCD1 would compromise the biological efficacy of dietary MR. Stated another way, we sought to understand whether MR-dependent suppression of hepatic SCD1 expression was a mediator of downstream effects of MR on energy balance and/or biomarkers of metabolism.

A key element of our experimental approach was to vary housing temperatures and examine mice housed near thermoneutrality to minimize the thermogenic response that is evident in WT mice under standard conditions (23 °C) (Cannon and Nedergaard 2004). This is an important design consideration because previous studies have shown that *Scd1*^{-/-} mice are significantly more cold-stressed than WT mice under these conditions and respond by increasing their energy intake and expenditure (Lee et al. 2004; Ntambi et al. 2002). Given that MR increases energy intake and expenditure in WT mice under standard conditions, we were uncertain whether MR would be able to produce additional effects on these variables when *Scd1*^{-/-} mice were housed at 23 °C. Figures 1A–1D illustrate that *Scd1*^{-/-} mice on the CON diet at 23 °C had the expected lower BW and adiposity, and higher energy intake and EE compared with WT mice. Notwithstanding these effects of the *Scd1*^{-/-} genotype alone, dietary MR produced an additional reduction in adiposity (Fig. 1B), an increase in energy intake (Fig. 1C), and an increase in EE (Fig. 1D) in *Scd1*^{-/-} mice at 23 °C that was

comparable to the responses in WT mice. These initial findings support our view that dietary MR is able to produce its metabolic phenotype in the absence of SCD1.

The second objective of this experiment was to test the efficacy of dietary MR in WT and *Scd1*^{-/-} mice reared at temperatures (e.g., 28 °C) that minimized sympathetic nervous system (SNS) activity and thermal stress (Gordon, 2012). Figure 1D illustrates that the shift from 23 °C to 28 °C produced the expected reductions in EE in both genotypes. For example, in WT mice on the CON diet, EE was 60% lower in mice reared at 28 °C compared with 23°C (Fig. 1D), and energy intake was 25% lower at the higher temperature (Fig. 1C). In parallel fashion, *Scd1*^{-/-} mice on the CON diet responded to the higher temperature with a 50% reduction in EE and a 15% reduction in energy intake (Figs. 1C, 1D). However, it was surprising to see that EE in *Scd1*^{-/-} mice on the CON diet remained significantly higher than WT mice on the CON diet (Fig. 1D). This genotypic difference extended to energy intake of the CON diet, where *Scd1*^{-/-} mice consumed significantly more calories than WT mice. A significant design limitation of the current experiment is that the effects of MR and housing temperature on energy balance in WT and *Scd1*^{-/-} mice were studied sequentially in the same mice. A better approach would have been to compare the responses to MR at the 2 housing temperatures in similarly aged cohorts of the 2 genotypes. Our previous work provides little evidence of a diet by age interaction with respect to the effects of MR on the variables examined in Fig. 1 (Hasek et al. 2010), although there are subtle differences in the way BW and adiposity are affected by MR in young versus older animals. For example, if MR is initiated soon after weaning (e.g., 5–6 weeks of age), MR slows the accretion of BW and adiposity compared with mice on the control diet. In contrast, when MR is initiated in rats that are close to their mature size, dietary MR tends to keep BW and adiposity unchanged while animals on the control diet continue to slowly add BW and fat (Hasek et al. 2010). As presently designed, the effects of housing temperature and genotype are confounded with the age of the mice when responses to the 2 diets were measured. Nevertheless, based on our previous work with the MR diet at different ages (Hasek et al. 2010) and housing temperatures (Wanders et al. 2015), we attribute the minimal energy balance responses of *Scd1*^{-/-} mice to the MR diet at 28 °C to be driven by a genotype by temperature interaction with minimal influence of age. Surprisingly, our findings suggest that *Scd1*^{-/-} mice on the CON diet were responding as if cold stressed, even under thermoneutral conditions. Similar findings were reported in mice with a skin-specific deletion of *Scd1*^{-/-} and housed at the high range of thermoneutral conditions (e.g., 33 °C) (Flowers et al. 2011; Sampath et al. 2009). The authors found that skin-specific *Scd1*^{-/-} mice had higher EE and accumulated significantly less BW despite consuming significantly more food (Flowers et al. 2011). Although EE was not measured in this study, their observations are consistent with a genotype-dependent increase in EE. Together, these findings suggest that mechanisms independent of thermal stress are driving the hypermetabolic phenotype of *Scd1*^{-/-} mice. Flowers et al. (2011) identified disturbed retinol metabolism as a potential contributor to the *Scd1*^{-/-} phenotype, but it is unclear at present whether dietary MR produces similar alterations.

The comparable increases in EE produced by dietary MR at 28 °C in WT and *Scd1*^{-/-} mice were matched by comparable increases in UCP1 protein in BAT and *Ucp1* mRNA in IWAT (Figs. 1E, 1F). However, these findings present an interesting dichotomy with respect to

genotypic comparisons of UCP1 expression levels and EE in mice on the CON diet. The similar expression levels of UCP1 in WT and *Scd1*^{-/-} mice on the CON diet argue that housing at 28 °C generates comparable SNS outflow to adipose tissue in each genotype (Figs. 1E, 1F). In contrast, EE is significantly higher in *Scd1*^{-/-} mice on the CON diet compared with WT mice (Fig. 1D). This difference suggests that the absence of SCD1 is affecting EE through a mechanism independent of upregulating SNS outflow to adipose tissue.

Our recent work established that FGF21 is a critical mediator of the effects of dietary MR on thermogenesis, white adipose tissue remodeling, and EE (Wanders et al. 2017), so it was somewhat surprising to observe that MR induced hepatic *Fgf21* mRNA to lower levels in *Scd1*^{-/-} compared with WT mice (Fig. 3A). However, it is also interesting that the absence of *Scd1*^{-/-} produced a significant decrease in hepatic *Fgf21* mRNA levels in mice on the CON diet (Fig. 3A). Peroxisome proliferator-activated receptor α (PPAR α) is an important transcriptional regulator of hepatic FGF21 expression (Inagaki et al. 2007). Given the decrease in hepatic unsaturated fatty acids in *Scd1*^{-/-} mice (Miyazaki et al. 2001a), perhaps a decrease in the production of PPAR α ligands lowers basal FGF21 expression in *Scd1*^{-/-} mice. Dietary MR is thought to induce hepatic FGF21 expression through a combination of mechanisms involving PKR-like ER stress kinase (PERK) and nuclear factor (erythroid-derived)-like 2 (NRF2)-dependent activation of activating transcription factor 4 (ATF4) recruitment to the FGF21 promoter (Wanders et al. 2016). Thus, even though basal *Fgf21* mRNA levels were lower in *Scd1*^{-/-} compared with WT mice, the fold-induction of FGF21 in the 2 genotypes was comparable (Fig. 3A). It is possible that a comparable fold-change in serum FGF21 is the key factor linking dietary MR to comparable thermogenic responses between the genotypes. This conclusion is supported by the similar induction of UCP1 in BAT and WAT by MR in the respective phenotypes (Figs. 1E, 1F). In contrast, the lack of an increase in energy intake and reduction in adiposity of *Scd1*^{-/-} mice on the MR diet may be reflective of the less robust induction of hepatic FGF21. It is also possible that the diet-independent effects of genotype on adiposity and energy intake may have limited additional effects of the MR diet.

Our recent work showed that the downregulation of hepatic SCD1 expression by dietary MR was intact in *Fgf21*^{-/-} mice while the upregulation of SCD1 in WAT, as well as the induction of thermogenic genes there, was dependent on FGF21 (Wanders et al. 2017). Therefore, we interpret these data to mean that the key response driving the MR-dependent increase in EE is the FGF21-mediated induction of thermogenic genes. Support for this conclusion comes from our earlier work with UCP1 null mice (Wanders et al. 2015), where MR induced hepatic FGF21 normally but was unable to increase EE, reduce BW, or reduce adiposity. Although not presented in our original findings (Wanders et al. 2015), MR was able to increase SCD1 expression in WAT in both WT and *Ucp1*^{-/-} mice. We interpret these findings to mean that the upregulation of SCD1 in WAT is not a key mediator of MR's effects on energy balance.

Several of the MR-dependent responses observed in WT mice were absent in *Scd1*^{-/-} mice. For example, the normal diet-induced increase in serum adiponectin and reductions in serum insulin and leptin were absent in *Scd1*^{-/-} mice (Figs. 3B, 3D). Recent studies established a

role for FGF21 in regulating transcription and release of adiponectin from adipose tissue (Holland et al. 2013; Lin et al. 2015). Thus, the failure of MR to increase plasma adiponectin in *Scd1*^{-/-} mice may be linked to the muted increase in FGF21 produced by the diet in these mice. In contrast, the failure of dietary MR to produce additional reductions in serum insulin or leptin is most likely the result of the strong diet-independent effect of genotype on these variables that makes little additional reduction possible. Serum leptin was reduced 3.7-fold by MR in WT mice, but was reduced 9.6-fold by the *Scd1*^{-/-} genotype independent of diet (Fig. 3D). A similar pattern was seen with serum insulin where the effect of the MR diet in WT mice was comparable to the effect of the *Scd1*^{-/-} genotype (Fig. 3C). Our previous work has shown that dietary MR increases in vivo insulin sensitivity through a combination of mechanisms involving reduced adiposity and FGF21 (Wanders et al. 2017; Stone et al. 2014). It seems likely that the diet-independent effect of the *Scd1*^{-/-} genotype to reduce adiposity was an important factor in reducing insulin and leptin levels, and that the failure of MR to further reduce adiposity limited its ability to produce further reductions in insulin or leptin. Collectively, the present findings fail to support the conclusion that MR-dependent reduction of hepatic SCD1 is a key mediator of the biological effects of dietary MR.

Acknowledgments

The authors acknowledge the excellent technical assistance of Nancy Van, Kelly Dille, and Mollye Baker, and the administrative support of Cindi Tramonte.

References

- Ables GP, Perrone CE, Orentreich D, Orentreich N. Methionine-restricted C57BL/6J mice are resistant to diet-induced obesity and insulin resistance but have low bone density. *PLoS ONE*. 2012; 7:e51357. eCollection 2014. doi: 10.1371/journal.pone.0051357 [PubMed: 23236485]
- Binczek E, Jenke B, Holz B, Gunter RH, Thevis M, Stoffel W. Obesity resistance of the stearoyl-CoA desaturase-deficient (*scd1*^{-/-}) mouse results from disruption of the epidermal lipid barrier and adaptive thermo-regulation. *Biol Chem*. 2007; 388:405–418. [PubMed: 17391062]
- Cannon B, Nedergaard J. Brown adipose tissue: function and physiological significance. *Physiol Rev*. 2004; 84:277–359. DOI: 10.1152/physrev.00015.2003 [PubMed: 14715917]
- Cohen P, Miyazaki M, Socci ND, Hagge-Greenberg A, Liedtke W, Soukas AA, et al. Role for stearoyl-CoA desaturase-1 in leptin-mediated weight loss. *Science*. 2002; 297:240–243. DOI: 10.1126/science.1071527 [PubMed: 12114623]
- Commings SP, Watson PM, Padgett MA, Dudley A, Argyropoulos G, Gettys TW. Induction of uncoupling protein expression in brown and white adipose tissue by leptin. *Endocrinology*. 1999; 140:292–300. DOI: 10.1210/endo.140.1.6399 [PubMed: 9886838]
- Dobrzyn P, Dobrzyn A, Miyazaki M, Cohen P, Asilmaz E, Hardie DG, et al. Stearoyl-CoA desaturase 1 deficiency increases fatty acid oxidation by activating AMP-activated protein kinase in liver. *Proc Natl Acad Sci USA*. 2004; 101:6409–6414. DOI: 10.1073/pnas.0401627101 [PubMed: 15096593]
- Flowers MT, Paton CM, O'Byrne SM, Schiesser K, Dawson JA, Blaner WS, et al. Metabolic changes in skin caused by *Scd1* deficiency: a focus on retinol metabolism. *PLoS ONE*. 2011; 6:e19734. doi: 10.1371/journal.pone.0019734 [PubMed: 21573029]
- Flowers MT, Ade L, Strable MS, Ntambi JM. Combined deletion of SCD1 from adipose tissue and liver does not protect mice from obesity. *J Lipid Res*. 2012; 53:1646–1653. DOI: 10.1194/jlr.M027508 [PubMed: 22669918]
- Gates AH, Karasek M. Hereditary absence of sebaceous glands in the mouse. *Science*. 1965; 148:1471–1473. DOI: 10.1126/science.148.3676.1471 [PubMed: 17738154]

- Gordon CJ. Thermal physiology of laboratory mice: Defining thermoneutrality. *J Therm Biol.* 2012; 37:654–685. DOI: 10.1016/j.jtherbio.2012.08.004
- Gutierrez-Juarez R, Pocai A, Mulas C, Ono H, Bhanot S, Monia BP, et al. Critical role of stearoyl-CoA desaturase-1 (SCD1) in the onset of diet-induced hepatic insulin resistance. *J Clin Invest.* 2006; 116:1686–1695. DOI: 10.1172/JCI26991 [PubMed: 16741579]
- Hasek BE, Stewart LK, Henagan TM, Boudreau A, Lenard NR, Black C, et al. Dietary methionine restriction enhances metabolic flexibility and increases uncoupled respiration in both fed and fasted states. *Am J Physiol.* 2010; 299:R728–R739. DOI: 10.1152/ajpregu.00837.2009
- Hasek BE, Boudreau A, Shin J, Feng D, Hulver M, Van N, et al. Remodeling the integration of lipid metabolism between liver and adipose tissue by dietary methionine restriction in rats. *Diabetes.* 2013; 62:3362–3372. DOI: 10.2337/db13-0501 [PubMed: 23801581]
- Holland WL, Adams AC, Brozinick JT, Bui HH, Miyauchi Y, Kusminski CM, et al. An FGF21-adiponectin-ceramide axis controls energy expenditure and insulin action in mice. *Cell Metab.* 2013; 17:790–797. DOI: 10.1016/j.cmet.2013.03.019 [PubMed: 23663742]
- Hyun CK, Kim ED, Flowers MT, Liu X, Kim E, Strable M, Ntambi JM. Adipose-specific deletion of stearoyl-CoA desaturase 1 up-regulates the glucose transporter GLUT1 in adipose tissue. *BBRC.* 2010; 399:480–486. DOI: 10.1016/j.bbrc.2010.07.072 [PubMed: 20655875]
- Inagaki T, Dutchak P, Zhao G, Ding X, Gautron L, Parameswara V, et al. Endocrine regulation of the fasting response by PPAR α -mediated induction of fibroblast growth factor 21. *Cell Metab.* 2007; 5:415–425. DOI: 10.1016/j.cmet.2007.05.003 [PubMed: 17550777]
- Lee SH, Dobrzyn A, Dobrzyn P, Rahman SM, Miyazaki M, Ntambi JM. Lack of stearoyl-CoA desaturase 1 upregulates basal thermogenesis but causes hypothermia in a cold environment. *J Lipid Res.* 2004; 45:1674–1682. DOI: 10.1194/jlr.M400039-JLR200 [PubMed: 15210843]
- Lin Z, Pan X, Wu F, Ye D, Zhang Y, Wang Y, et al. Fibroblast growth factor 21 prevents atherosclerosis by suppression of hepatic sterol regulatory element-binding protein-2 and induction of adiponectin in mice. *Circulation.* 2015; 131:1861–1871. DOI: 10.1161/CIRCULATIONAHA.115.015308 [PubMed: 25794851]
- Malloy VL, Krajcik RA, Bailey SJ, Hristopoulos G, Plummer JD, Orentreich N. Methionine restriction decreases visceral fat mass and preserves insulin action in aging male Fischer 344 rats independent of energy restriction. *Aging Cell.* 2006; 5:305–314. DOI: 10.1111/j.1474-9726.2006.00220.x [PubMed: 16800846]
- Miyazaki M, Kim YC, Gray-Keller MP, Attie AD, Ntambi JM. The biosynthesis of hepatic cholesterol esters and triglycerides is impaired in mice with a disruption of the gene for stearoyl-CoA desaturase 1. *J Biol Chem.* 2000; 275:30132–30138. DOI: 10.1074/jbc.M005488200 [PubMed: 10899171]
- Miyazaki M, Kim YC, Ntambi JM. A lipogenic diet in mice with a disruption of the stearoyl-CoA desaturase 1 gene reveals a stringent requirement of endogenous monounsaturated fatty acids for triglyceride synthesis. *J Lipid Res.* 2001a; 42:1018–1024. [PubMed: 11441127]
- Miyazaki M, Man WC, Ntambi JM. Targeted disruption of stearoyl-CoA desaturase1 gene in mice causes atrophy of sebaceous and meibomian glands and depletion of wax esters in the eyelid. *J Nutr.* 2001b; 131:2260–2268. [PubMed: 11533264]
- Miyazaki M, Flowers MT, Sampath H, Chu K, Otzelberger C, Liu X, Ntambi JM. Hepatic stearoyl-CoA desaturase-1 deficiency protects mice from carbohydrate-induced adiposity and hepatic steatosis. *Cell Metab.* 2007; 6:484–496. DOI: 10.1016/j.cmet.2007.10.014 [PubMed: 18054317]
- Ntambi JM, Miyazaki M, Stoehr JP, Lan H, Kendzioriski CM, Yandell BS, et al. Loss of stearoyl-CoA desaturase-1 function protects mice against adiposity. *Proc Natl Acad Sci USA.* 2002; 99:11482–11486. DOI: 10.1073/pnas.132384699 [PubMed: 12177411]
- Paton CM, Ntambi JM. Biochemical and physiological function of stearoyl-CoA desaturase. *Am J Physiol.* 2009; 297:E28–E37. DOI: 10.1152/ajpendo.90897.2008
- Perrone CE, Mattocks DA, Jarvis-Morar M, Plummer JD, Orentreich N. Methionine restriction effects on mitochondrial biogenesis and aerobic capacity in white adipose tissue, liver, and skeletal muscle of F344 rats. *Metabolism.* 2010; 59:1000–1011. DOI: 10.1016/j.metabol.2009.10.023 [PubMed: 20045141]

- Rahman SM, Dobrzyn A, Lee SH, Dobrzyn P, Miyazaki M, Ntambi JM. Stearoyl-CoA desaturase 1 deficiency increases insulin signaling and glycogen accumulation in brown adipose tissue. *Am J Physiol.* 2005; 288:E381–E387. DOI: 10.1152/ajpendo.00314.2004
- Sampath H, Flowers MT, Liu X, Paton CM, Sullivan R, Chu K, et al. Skin-specific deletion of stearoyl-CoA desaturase-1 alters skin lipid composition and protects mice from high fat diet-induced obesity. *J Biol Chem.* 2009; 284:19961–19973. DOI: 10.1074/jbc.M109.014225 [PubMed: 19429677]
- Stone KP, Wanders D, Orgeron M, Cortez CC, Gettys TW. Mechanisms of increased in vivo insulin sensitivity by dietary methionine restriction in mice. *Diabetes.* 2014; 63:3721–3733. DOI: 10.2337/db14-0464.PMID:24947368 [PubMed: 24947368]
- Wanders D, Burk DH, Cortez CC, Van NT, Stone KP, Baker M, et al. UCP1 is an essential mediator of the effects of methionine restriction on energy balance but not insulin sensitivity. *FASEB J.* 2015; 29:2603–2615. DOI: 10.1096/fj.14-270348 [PubMed: 25742717]
- Wanders D, Stone KP, Forney LA, Cortez CC, Dille KN, Simon J, et al. Role of GCN2-independent signaling through a noncanonical PERK/ NRF2 pathway in the physiological responses to dietary methionine restriction. *Diabetes.* 2016; 65:1499–1510. DOI: 10.2337/db15-1324 [PubMed: 26936965]
- Wanders D, Forney LA, Stone KP, Burk DH, Pierse A, Gettys TW. FGF21 mediates the thermogenic and insulin-sensitizing effects of dietary methionine restriction but not its effects on hepatic lipid metabolism. *Diabetes.* 2017; 66:858–867. DOI: 10.2337/db16-1212 [PubMed: 28096260]

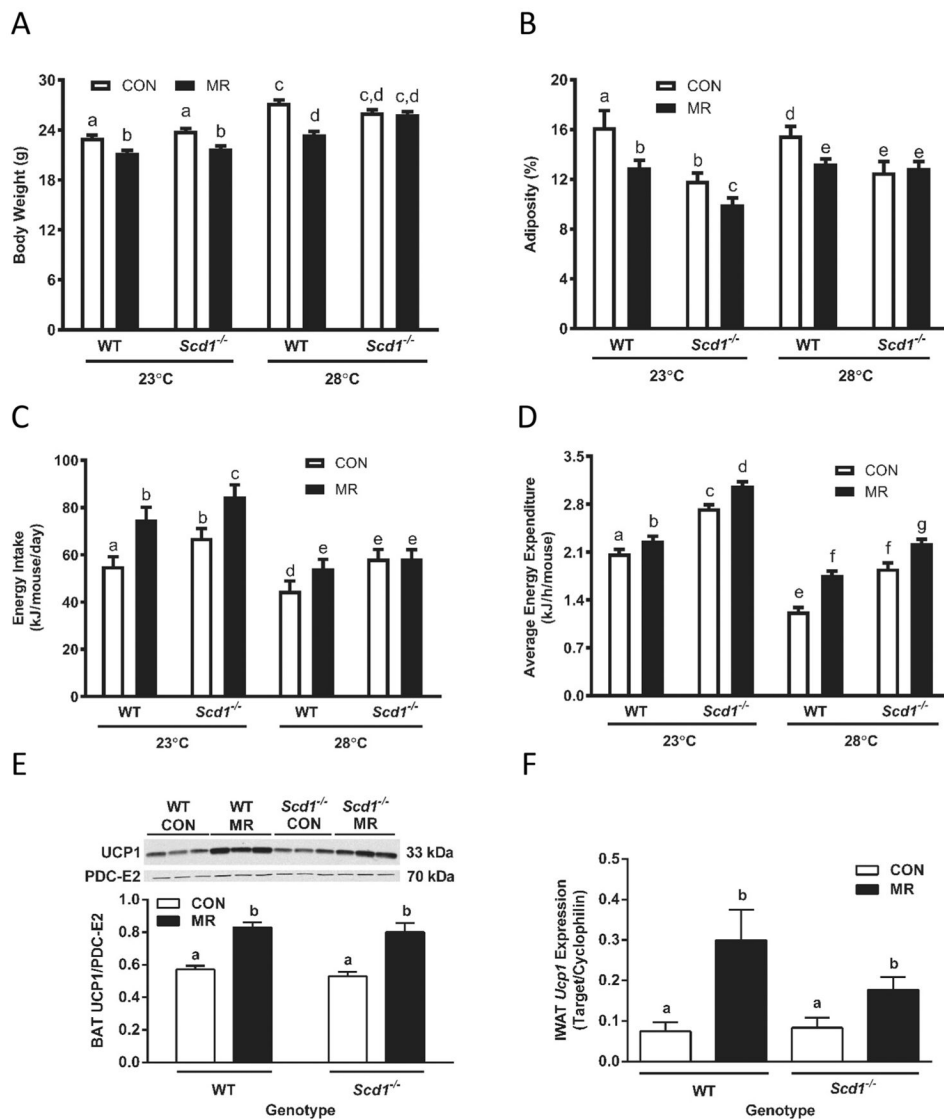


Fig. 1. Assessment of chronic effects of dietary methionine restriction (MR) on energy balance in wild-type (WT) and *stearoyl-coenzyme A desaturase-1* (*Scd1*^{-/-}) mice housed initially at 23 °C and then after transfer to 28 °C. Animals were housed at 23 °C and acclimated to the control (CON) diet for 1 week beginning at 5 weeks of age, after which half the mice of each genotype were randomized to receive the MR diet. Average body weight (A), adiposity (B), daily energy intake per mouse (C), and energy expenditure (D) were measured after 5 weeks on the respective diets. Thereafter the mice were housed at 28 °C for an additional 5 weeks and the responses presented in figure panels A–D were remeasured. In tissues harvested thereafter, brown adipose tissue (BAT) uncoupling protein-1 (UCP1) expression (E) was measured by Western blotting in cell lysates and standardized to pyruvate dehydrogenase complex E2 (PDC-E2), while IWAT *Ucp1* messenger RNA (mRNA) (F) was measured by real-time polymerase chain reaction and expressed relative to cyclophilin. Means ± SE of body weight, adiposity, and energy intake were measured after 5 weeks at

23 °C and 5 weeks at 28 °C, and means annotated with different letters differ at $P < 0.05$. Energy expenditure was measured after 5 weeks at 23 °C and 5 weeks at 28 °C, and least-square means \pm SE were calculated by ANCOVA as described in the Materials and methods section. BAT UCP1 protein expression and IWAT *Ucp1* mRNA were expressed as means \pm SE and means annotated with different letters differ at $p < 0.05$.

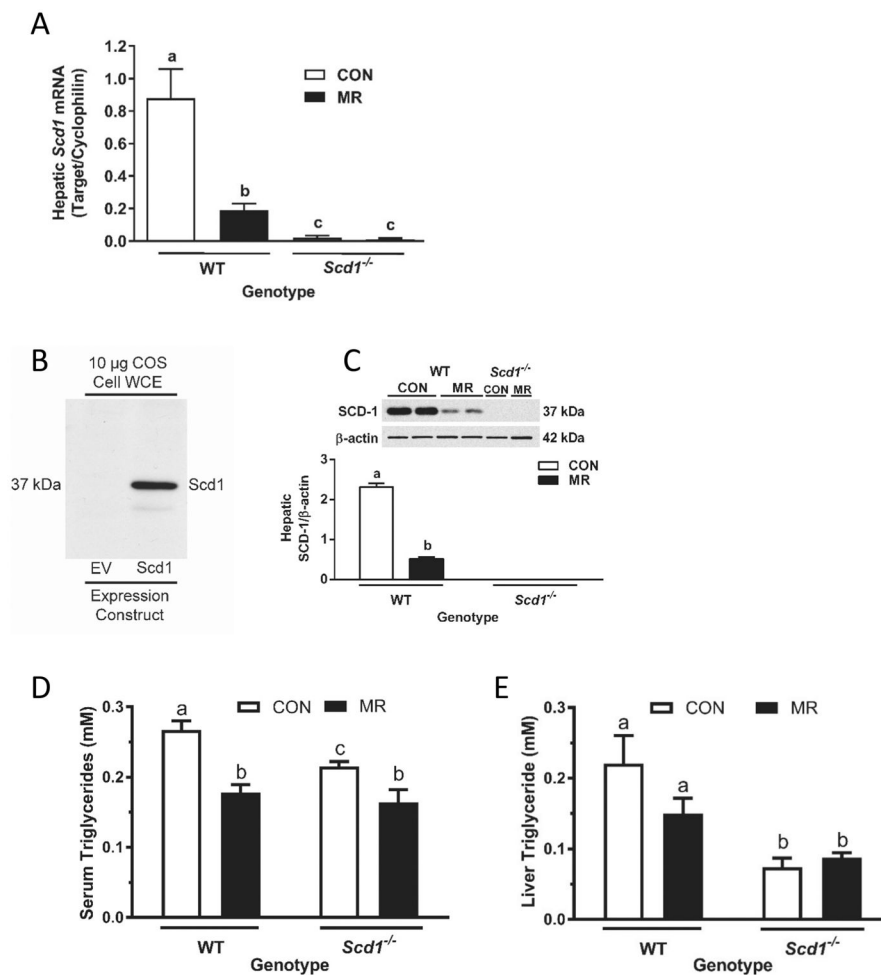


Fig. 2. Effects of dietary methionine restriction (MR) on hepatic stearoyl-coenzyme A desaturase-1 (SCD1) expression and liver and serum triglycerides in wild-type (WT) and *Scd1*^{-/-} mice. Hepatic *Scd1* messenger RNA (mRNA) (A) was measured via real-time polymerase chain reaction and standardized to cyclophilin. Whole-cell extracts (WCE) from COS cells transfected with empty vector (EV) or *Scd1* were analyzed by Western blot (B) to establish specificity of the antibody. Expression of SCD1 was determined in hepatic microsomes prepared from WT mice and *Scd1*^{-/-} mice. Lanes 1–4 in panel C are from WT mice, and are representative of 5 animals per diet, while lanes 5–6 from *Scd1*^{-/-} mice were included to establish absence of SCD1 expression in *Scd1*^{-/-} mice. SCD1 expression was normalized to β-actin and means annotated with different letters differ at $P < 0.05$ (C). Means \pm SE of serum (D) and hepatic (E) triglyceride were determined in 5 mice from each genotype and diet, and means annotated with different letters differ at $P < 0.05$. CON, control; mM, mmol/L.

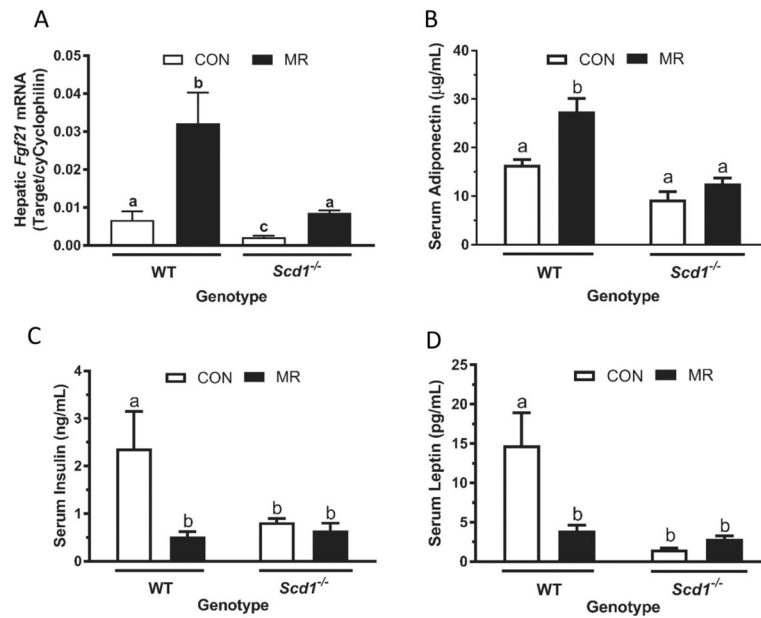


Fig. 3. Effects of dietary methionine restriction (MR) on hepatic *fibroblast growth factor-21* (*Fgf21*) and serum hormones in wild-type (WT) and *stearoyl-coenzyme A desaturase-1* (*Scd1*^{-/-}) mice. Hepatic *Fgf21* expression (A) and serum adiponectin (B), insulin (C), and leptin (D) were measured in samples harvested at study's end. *Fgf21* messenger RNA (mRNA) expression was determined using real-time polymerase chain reaction and standardized to cyclophilin expression. Serum adiponectin, insulin, and leptin were determined using enzyme-linked immunosorbent assays (ELISA). Data are expressed as means \pm SE from 5 mice of each genotype and diet combination, and means annotated with different letters differ at $P < 0.05$. CON, control.